

Microgrooved plasmonic bottle microresonator

M N Mohd Nasir, M Ding, G S Murugan, M N Zervas

Optoelectronics Research Centre, University of Southampton, Highfield,
Southampton, SO17 1BJ, UK.

E-mail: mnmn1r11@orc.soton.ac.uk

Abstract. In this paper, we demonstrate an enhancement to SPW cavity through the incorporation of high- Q WGM bottle microresonator (BMR) with surface microgrooves. A standard BMR fabricated through the “soften-and-compress” technique with initial length of $280\ \mu\text{m}$, bottle diameter of $187\ \mu\text{m}$ and stem diameter of $125\ \mu\text{m}$ was utilized in the experiment for supporting WGMs. Thin gold film was deposited on top of the BMR for generating SPWs. 21 microgrooves was then inscribed on the metal surface of the BMR along the azimuthal direction with $10\ \mu\text{m}$ length, $485\ \text{nm}$ width, $6\ \mu\text{m}$ depth and pitch of $1.5\ \mu\text{m}$. Due to surface curvature, the gold film only covered half of the BMR with a characteristic meniscus shape and maximum thickness of $30\ \text{nm}$. The meniscus provides appropriately tapered metal edges that facilitate the adiabatic transformation of BMR WGMs to SPWs and vice-versa. Lorentzian shape-line fit performed on the TM excited resonances show that plasmonic Q values in excess of 4000 could be achieved from such structure with $\sim 25\%$ coupling efficiency.

1. Introduction

The ability of surface plasmons in tailoring its interaction with light through the alteration of the metal's surface has opened up many great possibilities on the advancement of new types of photonics devices. However, in contrast to the high- Q factor of dielectric cavity resonators, surface plasmonic cavities performances has been reported to attain Q -factor values much lower than their theoretical values. The reported surface plasmonic cavity to date includes ring [1] and ring type v-groove [2], annular resonator [3], nanowire Fabry-Pérot (FP) [4] and periodic optical Bragg mirrors [5], [6]. The ability of whispering gallery (WG) structure in sustaining high- Q cavities has prompted extensive studies in the development of high- Q hybrid WGM-plasmonic microresonators. The demonstration of WG-plasmonic resonance in Au cylinder excited with tapered fibre has shown Q -factor value reaching the 300s [7]. A much more advanced WG dielectric microdisk resonator half-coated with silver has been demonstrated to attain Q -factor in excess of 1300 when excited from the dielectric side of the disk [8]. A study on WG microtoroid resonator coated with silver has also been anticipated to support plasmonic-WGMs with Q value reaching 1000s [9]. Recently we have proposed a high- Q hybrid plasmonic-BMR (PBMR) with a characteristic meniscus shape Au coating on top of the resonator [10]. TM-WGM excitation from the dielectric side of the plasmonic-BMR shows surface plasmon waves (SPWs) with composite Q -factor reaching 850 and individual Q -factor in excess of 2500 could be generated with coupling efficiency of $\sim 75\%$.

In this paper, we demonstrate another type of hybrid plasmonic-BMR with the incorporation of microgroove gratings on the surface of the resonator. 21 microgrooves inscribed on the metal surface of the PBMR is demonstrated to excite WGMs which are very different form the original BMR. TM-



excited WGMs is demonstrated to generate SPWs with Q -factor reaching 4000 and $\sim 25\%$ coupling efficiency.

2. Experimental setup

The BMR utilized in the experiment was fabricated using conventional silica fibre (SMF-28) through the “soften-and-compress” technique. As shown in figure 1 (a), the original BMR has initial bottle diameter D_b of $187\ \mu\text{m}$, length L_b of $280\ \mu\text{m}$ and stem diameter D_s of $125\ \mu\text{m}$. Original WGMs excited at the centre of the BMR with tapered fibre of $2\ \mu\text{m}$ waist diameter shows complex and dense spectra over a broad spectrum, as shown in figure 1 (b).

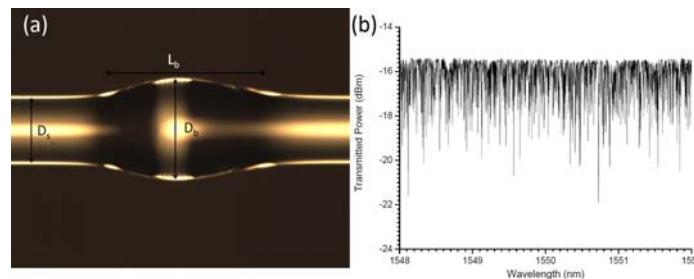


Figure 1 (a) BMR utilized before metal coating. (b) Initial BMR-WGMs excited at centre position.

The top surface of the BMR was then deposited with a thin gold layer. Due to the surface curvature of the BMR, the gold film only covered half of the resonator with a characteristic meniscus shape and maximum thickness of $30\ \text{nm}$. Adiabatic transformation of the BMR-WGMs into SPWs and vice-versa would be expedited by the tapered edges of the meniscus. Focused ion beam (FIB) milling with $50\ \text{nm}$ precision were utilized in the experiment in order to inscribe 21 microgrooves on the azimuthal direction of the BMR metal surface. The microgrooves were inscribed with length of $10\ \mu\text{m}$, width of $485\ \text{nm}$, depth of $6\ \mu\text{m}$ and pitch of $1.5\ \mu\text{m}$. Figure 2 (a) shows top side of the BMR with the scanning electron micrograph image of the microgrooves shown in figure 2 (b).

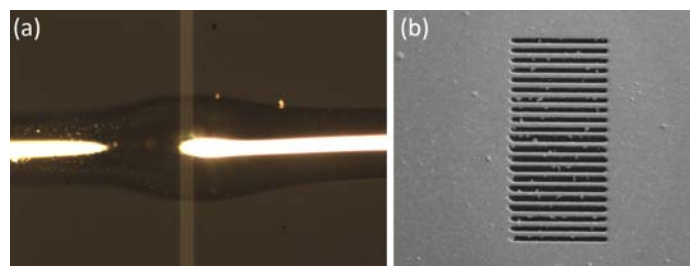


Figure 2 (a) Top side of the coated BMR with $30\ \text{nm}$ thick gold. (b) SEM image of the inscribed microgrooves at the centre of BMR metal surface.

Figure 3 shows the schematic of the polarization-resolved measurement setup developed for characterizing the fabricated PBMR. A $2\ \mu\text{m}$ tapered fibre was utilized in the experiment in order to couple light from a tuneable laser source (TLS) into the cavity of the PBMR. Since the decay length of light is high into the metal, the coupling was performed at the dielectric part of the resonator [8], [11]. To excite the PBMR with different light input polarizations, a polarization controller was placed in the system after the TLS with a high-extinction ratio polarizer ($> 50\ \text{dB}$) placed after the coupling point. Micro positioning stages were utilized in the experiment for precise control of the PBMR coupling with the tapered fibre. The tapered fibre was cleaved at the full fibre diameter and brought in contact with the cavity by placing it on top of the resonator. A collimator was placed after the cleaved fibre in order to collimate the output light before it is aligned to pass through the polarizer. The polarizer was placed in the system in a manner where it could be freely rotated to 360° . The output light was then focused into a fiber using a fibre launcher setup and measured using an InGaAs optical power meter

for WGMs observation. The inset of figure 3 shows the scattering of light of the PBMR with an IR camera.

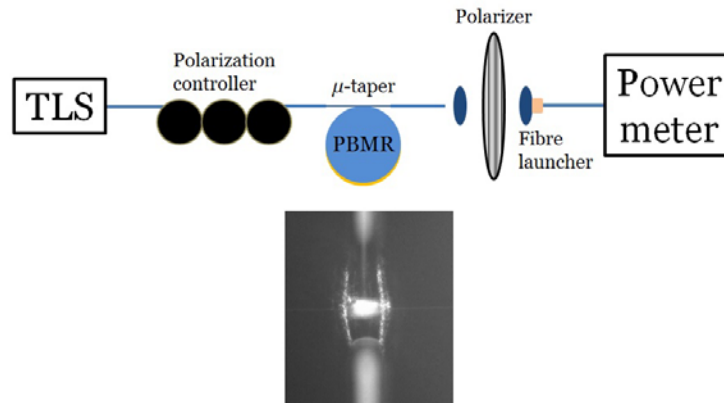


Figure 3. Schematic of the polarization-resolved measurement set-up for characterizing the fabricated PBMR with inset showing light scattering of the centrally excited PBMR.

3. Results and Discussion

The microtaper was coupled to the centre position of the dielectric part of the PBMR. The polarizer was then set to launch TE-polarized light into the cavity of the resonator. Figure 5 (a) shows the output resonance spectra of the TE-excited modes with maximum coupling efficiency of $\sim 80\%$ observed. The transmission spectra of the hybrid PBMR are dramatically different from the uncoated BMR as in figure 1 (b). Distinguishable family group-modes could also be observed from the output spectra with free spectral range (FSR) of ~ 2.9 nm; which matches the azimuthal resonances of the BMR. Fitting Lorentzian-shaped curves on the measured data revealed that the spectra actually comprise of overlapping resonances with higher Q value, as shown in Figure 5 (b). Maximum Q calculated is at resonance around 1550.2 nm with value of ~ 13000 .

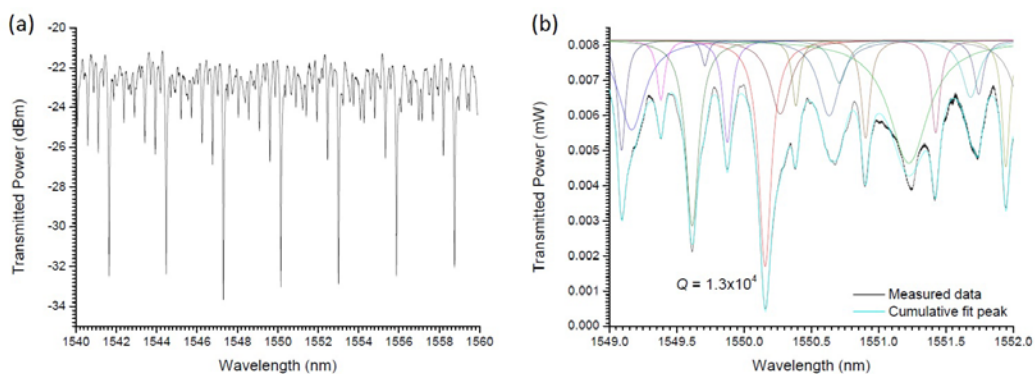


Figure 5 (a). Measured TE excited transmission spectra and (b) its Lorentzian-shaped curve fit.

Since SPWs are transverse magnetic in character, they require TM-polarized light as the source of excitation for electron density oscillations at the metal-dielectric interface. The polarization controller was then set to launch TM-polarized light into the cavity of the resonator. The output spectra observed shows maximum coupling efficiency is $\sim 25\%$, as shown in Figure 6 (a). The low transmission depth of the resonances is mainly due to light loss into the metal as they interact. Distinguishable family group-modes of FSR ~ 2.9 nm were also observed from the spectra. Figure 6 (b) illustrates the Lorentzian-shaped curves fit of the TM-excited modes. From the fitting, the output spectra actually comprise of multiple overlapping resonances with narrower individual resonances. The strongest

resonance dip which is at around 1556.1 nm has been calculated to attain Q in the range of 4700. However, the cumulative Q of the overlapping composite resonances at this wavelength is much lower, which is in the range of 700.

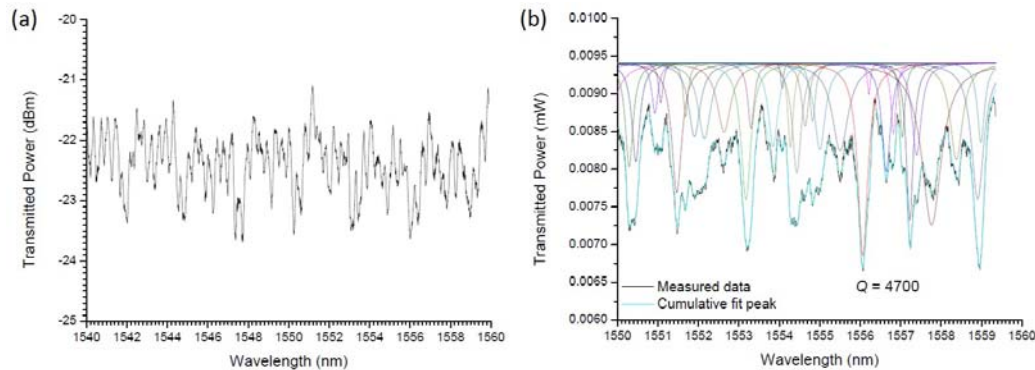


Figure 6 (a). Measured TM excited transmission spectra and (b) its Lorentzian-shaped curve fit.

4. Conclusion

We have studied experimentally the transmission properties of a microgrooved PBMR. An accurate polarization resolved measurement was developed in order to fully characterize the hybrid resonator. Different light polarization (TE and TM) coupled into the cavity of the resonator demonstrated that different modes are being excited by the cavity. Due to higher losses caused by SPWs, it was observed that TM-excited modes exhibited lower Q than TE-excited modes. Lorentzian-shaped curve fitting performed on the measured data reveals that TE/TM excitations are actually composite resonances comprising of multiple individual peaks with Q s in the range of 13000 and 4700, respectively.

References

- [1] S. I. Bozhevolnyi, V. S. Volkov, E. Devaux, J.-Y. Laluet, and T. W. Ebbesen, "Channel plasmon subwavelength waveguide components including interferometers and ring resonators," *Nature* **440**, 508-511 (2006).
- [2] A. Vardanyan, H. Haroyan, A. Babajanyan, K. Nerkararyan, and B. Friedman, "Ring-type V-groove surface plasmon microresonator: The modal structure and Q-factor," *Journal of Applied Physics* **111**, 053112 (2012).
- [3] C. E. Hofmann, E. J. R. Vesseur, L. A. Sweatlock, H. J. Lezec, F. J. García de Abajo, A. Polman, and H. A. Atwater, "Plasmonic Modes of Annular Nanoresonators Imaged by Spectrally Resolved Cathodoluminescence," *Nano Letters* **7**, 3612-3617 (2007).
- [4] H. Ditlbacher, A. Hohenau, D. Wagner, U. Kreibig, M. Rogers, F. Hofer, F. R. Aussenegg, and J. R. Krenn, "Silver Nanowires as Surface Plasmon Resonators," *Physical Review Letters* **95**, 257403 (2005).
- [5] J.-C. Webber, Y. Lacroute, A. Dereux, E. Devaux, T. Ebbesen, C. Girard, M. U. González, and A.-L. Baudrion, "Near-field characterization of Bragg mirrors engraved in surface plasmon waveguides," *Physical Review B* **70**, 235406 (2004).
- [6] J.-C. Webber, A. Bouhelier, G. C. des Francs, L. Markey, and A. Dereux, "Submicrometer In-Plane Integrated Surface Plasmon Cavities," *Nano Letters* **7**, 1352-1359 (2007).
- [7] X. Zhang, Z. Ma, H. Yu, X. Guo, Y. Ma, and L. Tong, "Plasmonic resonance of whispering gallery in an Au cylinder," *Optics Express* **19**, 3902-3907 (2011).
- [8] B. Min, E. Ostby, V. Sorger, E. Ulin-Avila, L. Yang, X. Zhang, and K. Vahala, "High-Q surface-plasmon-polariton whispering-gallery microcavity," *Nature* **457**, 455-459 (2009).
- [9] Y.-F. Xiao, C.-L. Zou, B.-B. Li, Y. Li, C.-H. Dong, Z.-F. Han, and Q. Gong, "High-Q Exterior Whispering-Gallery Modes in a Metal-Coated Microresonator," *Physical Review Letters* **105**, 153902 (2010).
- [10] M. N. Mohd Nasir, M. Ding, G. S. Murugan, and M. N. Zervas, "High-Q Plasmonic Bottle Microresonator," *Proceedings of SPIE* **8960**, 89600M (2014).
- [11] W. L. Barnes, A. Dereux, and T. W. Ebbesen, "Surface plasmon subwavelength optics," *Nature* **424**, 824-830 (2003).